

A Kinetic Investigation of Carbon Dioxide Insertion Processes Involving Anionic Tungsten-Alkyl and -Aryl Derivatives: Effects of CO₂ Pressure, Counterions, and Ancillary Ligands. Comparisons with Migratory Carbon Monoxide Insertion Processes

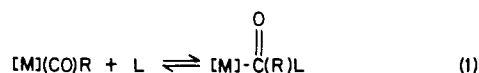
Donald J. Darensbourg,* Rebecca Kudasroski Hanckel, Christopher G. Bauch, Magdalena Pala, Debra Simmons, and J. Nicole White

Contribution from the Department of Chemistry, Texas A&M University, College Station, Texas 77843. Received May 31, 1985

Abstract: A mechanistic investigation of the 1,2-addition of carbon dioxide to tungsten-alkyl and -aryl derivatives, namely *cis*-RW(CO)₄L⁻ (R = Me, Et, and Ph; L = CO, PMe₃, and P(OMe)₃), to provide metallocarboxylates is reported. The reaction is shown to obey second-order kinetics, first order in anionic metal substrate and first order in carbon dioxide. A concerted reaction pathway involving an attack of the nucleophilic RW(CO)₅⁻ ion at the electrophilic carbon or carbon oxygen center of CO₂ is proposed. This proposal is supported by the dependence of the rate of these reactions on carbon monoxide and the nature of the metal center, the activation parameters, and the observed retention of configuration at the α-carbon atom. Replacement of carbon monoxide in the metal's coordination sphere by more electron-donating phosphite or phosphine ligands results in a significant enhancement of the rate of CO₂ insertion into the tungsten-carbon bond. For example, the rate of CO₂ insertion into *cis*-CH₃W(CO)₄PMe₃⁻ is 243 times greater than that in CH₃W(CO)₅⁻. The molecular structure of [PPN][*cis*-CH₃W(CO)₄PMe₃] was determined at -99 °C and W-CH₃ bond distance of 2.18 (3) Å was found to be somewhat shorter than that seen in the isoelectronic neutral Re-CH₃ analogue (2.308 (17) Å). The compound crystallizes in the monoclinic space group *Cc* with *a* = 16.538 (8) Å, *b* = 17.102 (9) Å, *c* = 16.106 (7) Å, β = 115.26 (3)°, and *V* = 4119.7 Å³. Unlike the carbon dioxide insertion reactions which did not exhibit a large rate dependence on the nature of the R group, migratory carbon monoxide insertion reactions involving these anionic RW(CO)₅⁻ derivatives display significant retardation with decreasing electron-donating ability of the R substituent. Further mechanistic comparisons of carboxylation and carbonylation processes are provided.

One of the most prominent class of reactions in organometallic chemistry is the insertion of small molecules into transition metal-alkyl or -aryl bonds to afford 1,1- or 1,2-addition products.¹ These reactions are pivotal steps in a large variety of important stoichiometric and catalytic processes, including polymerization of olefins, carbonylation of alcohols, Fischer-Tropsch and related syn gas chemistry, and hydroformylation.²

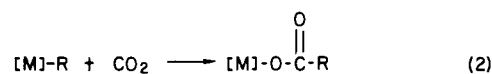
Migratory carbon monoxide insertion reactions which lead to 1,1-addition products (eq 1) are mechanistically the most well-characterized.³ Common features of these reactions are that they



proceed intramolecularly via R group migration with retention of configuration at the α-carbon atom. Further, kinetic studies demonstrate that these processes are accelerated by donating solvents and are highly dependent on the nature of R, with electron-withdrawing R groups retarding carbonylation and sterically bulky R groups enhancing carbonylation.⁴

By way of contrast, mechanistic investigations of the 1,2-addition of carbon dioxide to metal-alkyls and -aryls (eq 2) have received little attention.⁵ Nevertheless, this process constitutes

a fundamental step in the utilization of carbon dioxide as a viable feedstock in the production of organic substances. For example, transition-metal complexes have proved very useful in both the catalytic and stoichiometric production of cyclic lactones.⁶



Earlier studies from our laboratory have indicated that reaction 2 obeys second-order kinetics, first-order in metal substrate and first-order in carbon dioxide, and displays a dramatic rate enhancement upon increasing the electron density at the metal center as affected by the ancillary ligands.^{7,8} The metal substrates examined in these investigations were the anionic group 6B metal carbonyl alkyl and aryl derivatives, RM(CO)₅⁻ (M = Cr, W). It is anticipated that these anionic substrates will become paradigmatic for carboxylation reactions as their isoelectronic neutral analogues, RM(CO)₅ (M = Mn, Re), are for carbonylation processes. Unlike the neutral RMn(CO)₅ analogue which readily undergoes CO insertion but not CO₂ insertion,⁹ these anionic substrates sustain both carbonylation and carboxylation reactions at similar reaction conditions. Hence, these derivatives offer the distinct opportunity for comparative investigations of reactions 1 and 2 employing common substrates. We wish to report herein investigations aimed at providing a more comprehensive understanding of these carboxylation processes, as well as furnishing comparisons with the carbonylation reaction.

Experimental Section

All manipulations were carried out either in an argon drybox or on a double manifold Schlenk vacuum line, using freshly distilled solvents. Reagent grade tetrahydrofuran, hexane, toluene, and dimethoxyethane

(1) Alexander, J. In "Chemistry of the Metal-Carbon bond Stage 2"; Patai, S., Hartley, F. R., Eds.; Wiley: New York, 1983.

(2) Henrici-Olive, G.; Olive, S. "Coordination and Catalysis"; Verlag Chemie: New York, 1977.

(3) (a) Wojcicki, A. *Adv. Organomet. Chem.* **1973**, *11*, 87. (b) Wojcicki, A. *Adv. Organomet. Chem.* **1974**, *12*, 31. (c) Calderazzo, F. *Angew. Chem., Int. Ed. Engl.* **1977**, *16*, 299. (d) Kuhlmann, E. J.; Alexander, J. J. *Coord. Chem. Rev.* **1980**, *33*, 195. (e) Flood, T. C. *Top. Inorg. Organomet. Stereochem.* **1981**, *12*, 37.

(4) Cawse, J. N.; Fiato, F. A.; Pruett, R. L. *J. Organomet. Chem.* **1979**, *172*, 405.

(5) (a) Eisenberg, R.; Henderiksen, D. E. *Adv. Catal.* **1979**, *28*, 79. (b) Sneed, R. P. A. In "Comprehensive Organometallic Chemistry"; Wilkinson, G., Stone, F. G. A., Abel, E. W., Eds.; Pergamon Press: Oxford, 1982; Vol. 8, p 225. (c) Ito, T.; Yamamoto, A. "Organic and Bio-Organic Chemistry of Carbon Dioxide"; Inoue, S., Yamazaki, N., Eds.; Kodonsha, Ltd.: Tokyo, Japan, 1982, p 79. (d) Darensbourg, D. J.; Kudasroski, R. *Adv. Organomet. Chem.* **1983**, *22*, 129.

(6) (a) Albano, P.; Aresta, M. *J. Organomet. Chem.* **1980**, *190*, 243. (b) Tsuda, T.; Chiyo, Y.; Saegusa, T. *Synth. Commun.* **1979**, *9*, 427. (c) Dohring, A.; Jolly, P. W. *Tetrahedron Lett.* **1980**, *21*, 3021.

(7) Darensbourg, D. J.; Rokicki, A. *J. Am. Chem. Soc.* **1982**, *104*, 349.

(8) Darensbourg, D. J.; Kudasroski, R. *J. Am. Chem. Soc.* **1984**, *106*, 3672.

(9) Abel, E. W.; Butler, I. S.; Reid, J. G. *J. Chem. Soc.* **1963**, 2068.

were purified by distillation under nitrogen from sodium benzophenone ketyl. Dichloromethane and acetonitrile were refluxed under nitrogen over phosphorus pentoxide and distilled prior to use. Cr(CO)₆, W(CO)₆, trimethylphosphine, trimethyl phosphite, and bis(triphenylphosphine)iminium chloride were purchased from Strem Chemicals Inc. Methyl-lithium (low halide in diethyl ether), phenyllithium (in cyclohexane-ether 70:30), sodium tetraphenylborate, silver *p*-toluenesulfonate, methyl *p*-toluenesulfonate, ethyl *p*-toluenesulfonate, sodium propionate, and trimethylamine *n*-oxide were obtained from Aldrich Chemical Co. Phenol and *p*-toluenesulfonyl chloride were acquired from Matheson, Coleman, and Bell.

[PPN][M(CO)₅Cl] (M = Cr, W),⁹ M(CO)₅NHC₅H₁₀ and *cis*-M(CO)₄(NHC₅H₁₀)₂ (M = Cr, W),^{10,11} W(CO)₄(NHC₅H₁₀)(PR₃) (R = Me, OMe),¹¹ W(CO)₅NMe₃,¹² phenyl *p*-toluene sulfonate,¹³ and [PPN][O₂CCH₃]¹⁴ were prepared according to published procedures. Elemental analyses were carried out by Galbraith Laboratories. Infrared spectra were recorded on either a Perkin-Elmer 283B or an IBM FTIR/85 spectrometer. Proton and ¹³C NMR spectra were determined on a Varian XL-200 spectrometer. The ¹³C NMR spectra were recorded at 50.309 MHz in the absence of relaxation reagents employing a sweep width of 11 kHz with an acquisition time of 1.45 s, a pulse repetition rate of 5.45 s, and a flip angle of 33°.

Preparations

[PPN][tosylate]. Since the sodium salts of [*cis*-W(CO)₄(PR₃)R']⁻ proved to be very reactive toward halide ions present in solution, conversion of these sodium salts to the corresponding PPN⁺ salts required the use of bis(triphenylphosphine)iminium *p*-toluenesulfonate which was synthesized in the following manner.

[PPN][Cl] (6.07 g, 1.06 mmol) and silver *p*-toluenesulfonate (3.00 g, 1.08 mmol) were each dissolved in a minimum quantity of acetonitrile. The chloride solution was then slowly added to the silver *p*-toluenesulfonate solution with rapid stirring, where upon, AgCl precipitated and was removed by filtration. Acetonitrile was removed by vacuum distillation at ambient temperature leaving behind a pale yellow solid. Recrystallization from CH₂Cl₂/hexane afforded a white crystalline product (4.4 g) in 60% yield which was vacuum dried overnight.

[PPN][O₂CCH₂CH₃]. [PPN][Cl] (10.0 g, 17.4 mmol) dissolved in a minimum quantity of warm water was added to an aqueous solution of NaO₂CC₂H₅ (39.2 g, 410 mmol). The resulting solution was stirred for 2 h at ambient temperature, followed by standing at 10 °C overnight to provide a white precipitate. The product was isolated by filtration, washed with ice water, and recrystallized from warm diethyl ether.

[PPN][W(CO)₅R] (R = CH₃, C₆H₅). The complexes were prepared according to the published procedures.¹⁵ A typical preparation of [PPN][W(CO)₅CH₃] is described herein. [PPN][W(CO)₅Cl] (4.00 g, 4.46 mmol) dissolved in 30 mL of THF provided a golden yellow solution to which was added via syringe 0.5-mL aliquots of CH₃Li solution (1.25 M in diethyl ether). After each addition the progress of the reaction was monitored by the disappearance of the ν(CO) infrared band of the starting material at 1915 cm⁻¹. Complete conversion required approximately 4.0 mL (5 mmol) of the CH₃Li solution. Excess alkyllithium reagent was quenched by the addition of 10 mL of aqueous NaOH (1 N). The THF was removed by vacuum distillation and the tacky crude product which remained was washed with several 30-mL portions of distilled, deoxygenated water to remove the alkali metal salts. After vacuum drying overnight the product was recrystallized from THF/hexane to afford a lemon yellow solid. Anal. Calcd for C₄₂H₃₃NO₅P₂W: C, 57.49; H, 3.79; N, 1.60. Found: C, 57.51; H, 3.75; N, 1.57. The infrared spectrum in the ν(CO) region in THF is tabulated in Table I. ¹³C NMR (THF-*d*₈) δ 208.1 (CO_{ax}), 207.5 (CO_{eq}).

[PPN][W(CO)₅C₆H₅] was prepared in a similar manner from [PPN][W(CO)₅Cl] (4.00 g, 4.46 mmol) and C₆H₅Li (3.5 mL

Table I. Infrared Spectra in the ν(CO) Region of [PPN][*cis*-RM(CO)₄[L] Derivatives in Tetrahydrofuran Solution

M	L	R	ν(CO), ^a cm ⁻¹		
Cr	CO	CH ₃	2012 (w)	1887 (s)	1840 (m)
		O ₂ CCH ₃	2058 (w)	1920 (s)	1845 (m)
W	CO	CH ₃	2028 (w)	1883 (s)	1834 (m)
		C ₂ H ₅	2026 (w)	1882 (s)	1826 (m)
		CH ₂ CH ₂ -	2028 (w)	1885 (s)	1855 (m)
		C ₆ H ₅			
		C ₆ H ₅	2037 (w)	1894 (s)	1850 (m)
		O ₂ CCH ₃	2059 (w)	1907 (s)	1842 (m)
PMe ₃		O ₂ CC ₂ H ₅	2058 (w)	1910 (s)	1845 (m)
		CH ₃	1970 (w)	1845 (s)	1796 (m)
		C ₂ H ₅	1977 (w)	1850 (s)	1795 (m)
		O ₂ CCH ₃	1995 (w)	1872 (s), 1851 (s)	1979 (m)
P(OMe) ₃		CH ₃	1982 (w)	1855 (s)	1805 (m)
		C ₂ H ₅	1990 (w)	1965 (s)	1810 (m)
		C ₆ H ₅	1993 (w)	1869 (s)	1825 (m)
		O ₂ CCH ₃	2006 (w)	1885 (s), 1869 (s)	1811 (m)

^aFrequencies are accurate to ±1.0 cm⁻¹.

of 1.5 M solution). The infrared spectrum in the ν(CO) region in THF is tabulated in Table I. ¹³C NMR (THF-*d*₈) δ 207.8 (CO_{ax}), 204.9 (CO_{eq}).

[PPN][W(CO)₅C₂H₅].^{16,17} A solution of W(CO)₅NMe₃ (1.06 g, 2.77 mmol) in 30 mL of THF, cooled to -78 °C, was titrated with sodium naphthalinide (0.14 M in THF) until the green color persisted, generating Na₂W(CO)₅. Ethyl *p*-toluenesulfonate (0.5 mL, 2.9 mmol) was then added and the solution was allowed to warm up slowly to ambient temperature. After the addition of [PPN][tosylate] (2.0 g, 1.77 mmol) the solution was filtered through Celite. The filtrate was reduced in volume to one-half its original quantity and the product was precipitated upon the addition of 30 mL of hexane. The solid was washed with two 20-mL portions of hexane to provide a dark yellow powder. The product was further purified by washing three times with 20 mL of deoxygenated water to remove any remaining alkali metal salts followed by drying in vacuo, and finally recrystallization from THF/hexane.

[PPN][W(CO)₅CH₂CH₂C₆H₅] was prepared in an analogous manner. A sandy yellow material was obtained upon ion exchange with [PPN][Cl]. Infrared spectra in the ν(CO) region in THF solution are tabulated in Table I.

Cr(CO)₅(NHC₅H₁₀) (1.0, g 3.61 mmol) was dissolved in 25 mL of THF in a 100-mL Schlenk flask and cooled to -78 °C in a dry ice/acetone bath. This yellow solution was then titrated by syringe with a sodium naphthalinide solution (~35 mL of a 0.2 M THF solution) until the green color remained, generating Na₂Cr(CO)₅. A solution of methyl bromide (0.54 g in 3 mL of THF) was added to the reaction solution followed by the addition of [PPN][Cl] (2.3 g in 20 mL of CH₂Cl₂). The reaction mixture was then allowed to warm up to room temperature and all solvents were removed by vacuum distillation. The resulting sticky material was crystallized from THF/hexane to yield a yellow solid which was identified by infrared spectroscopy to be [PPN][Cr(CO)₅CH₃] contaminated with a small quantity of [PPN][Cr(CO)₅Br] (≤10%). This mixture was used for subsequent CO₂ insertion reactions. The infrared spectrum in the ν(CO) region is tabulated in Table I.

[PPN][*cis*-W(CO)₄(PR₃)R'] (R = Me; OMe; R' = CH₃, C₂H₅, C₆H₅). These complexes were all prepared from the corresponding *cis*-W(CO)₄[PR₃][NHC₅H₁₀] derivatives. A closely related synthesis of the *cis*-W(CO)₄[PR₃]H⁻ derivatives has previously been published.¹⁸

In a typical synthesis a solution of W(CO)₄P(OMe)₃(NC₅H₁₀) (0.5 g, 1.0 mmol) in 20 mL of THF cooled to -78 °C was titrated by syringe with sodium naphthalinide (0.14 M in THF) until the

(10) Dennenberg, R. J.; Darensbourg, D. J. *Inorg. Chem.* **1972**, *11*, 72.

(11) Darensbourg, D. J.; Kump, R. L. *Inorg. Chem.* **1978**, *17*, 2680.

(12) Strohmeier, W.; Guttenberger, J. F.; Blumenthal, H.; Albert, G. *Chem. Ber.* **1966**, *99*, 3419.

(13) Wentworth, S. E.; Sciaraffa, P. L. *Org. Prep. Proced.* **1979**, *1*, 225.

(14) Martinsen, A.; Songstad, J. *Acta Chem. Scand., Ser. A* **1977**, *A31*, 645.

(15) Casey, C. P.; Polichnowski, S. W. *J. Am. Chem. Soc.* **1978**, *100*, 7565.

(16) Ellis and Hagen¹⁷ have described a similar synthesis of this and related species, including those of chromium.

(17) Ellis, J. E.; Hagen, G. P. *Inorg. Chem.* **1977**, *16*, 1357.

(18) Slater, S. G.; Lusk, R.; Schumann, B. F.; Darensbourg, M. *Organometallics* **1982**, *1*, 1662.

green color remained to generate $\text{Na}_2\text{W}(\text{CO})_4\text{P}(\text{OMe})_3$.¹⁹ Methyl tosylate (0.20 g, 1.1 mmol) was then added and the solution was allowed to warm slowly to room temperature. After the addition of $[\text{PPN}][\text{tosylate}]$ (0.71 g, 1 mmol) the solution was filtered through Celite under nitrogen to remove the precipitated salts. The filtrate was then reduced to half volume and the crude product was isolated by the addition of 40 mL of hexane. The yellow solid was washed with 40 mL of toluene and recrystallized from THF/hexane. Yield: 0.55 g (57%).

$[\text{PPN}][\text{W}(\text{CO})_4(\text{PMe}_3)\text{CH}_3]$ was prepared by the same method but with the omission of the toluene wash. Yield: 0.58 g (63%). Crystals suitable for X-ray analysis were grown from THF/toluene/hexane (1:1:1) at 0 °C.

Both phosphine-substituted methyl complexes were found to be moderately air and moisture sensitive solids and, therefore, required storage and handling in a nitrogen or argon atmosphere. Completely analogous procedures were employed in the synthesis of the $[\text{PPN}][\text{cis-W}(\text{CO})_4(\text{L})\text{R}]$ (L = PMe_3 , $\text{P}(\text{OMe})_3$; R = C_2H_5 , C_6H_5) derivatives. Infrared spectra for all these species in the $\nu(\text{CO})$ region are listed in Table I.

$[\text{PPN}][\text{W}(\text{CO})_5(\text{O}_2\text{CC}_2\text{H}_5)]$. A solution of $[\text{PPN}][\text{O}_2\text{CC}_2\text{H}_5]$ (0.49 g, 0.81 mmol) and $\text{W}(\text{CO})_6$ (0.26 g, 0.74 mmol) in 20 mL of dimethoxyethane was refluxed for 2 h. The solvent was removed by vacuum distillation affording a dark yellow oil which was washed twice with 15-mL portions of hexane. Recrystallization from THF/hexane produced bright yellow crystals of the desired product. The infrared spectrum in the $\nu(\text{CO})$ region is tabulated in Table I.

$[\text{PPN}][\text{M}(\text{CO})_5(\text{O}_2\text{CCH}_3)]$ (M = Cr, W).^{20a} Silver acetate (2.61 mmol) was added to a dichloromethane solution of the appropriate halide, $[\text{PPN}][\text{M}(\text{CO})_5\text{Cl}]$ (1.88 mmol). After being stirred for 15 min, the solution was filtered under nitrogen through Celite, and the solvent was removed by vacuum distillation. The resulting yellow solid was recrystallized from THF/hexane.

Alternatively, these carboxylate derivatives were prepared from $\text{M}(\text{CO})_6$ and $[\text{PPN}][\text{acetate}]$ as described above for the propionate complex.

$[\text{PPN}][\text{cis-W}(\text{CO})_4(\text{L})(\text{O}_2\text{CCH}_3)]$ (L = PMe_3 , $\text{P}(\text{OMe})_3$).^{20b} To a solution of $[\text{PPN}][\text{W}(\text{CO})_5\text{O}_2\text{CCH}_3]$ (0.86 g, 0.94 mmol) in 30 mL of THF was added 2.04 mmol of the appropriate phosphine or phosphite ligand. The reaction mixture was heated at 50 °C for 1 h, cooled, and filtered through Celite under nitrogen. Bright yellow products were precipitated by the addition of 60 mL of hexane. Yields ranged from 75 to 82%.

$[\text{PPN}][\text{W}(\text{CO})_5\text{C}(\text{O})\text{CH}_3]$. Methyl lithium (1.5 mL of 1.1 M in Et_2O , 1.65 mmol) was added to a solution of $\text{W}(\text{CO})_6$ (0.373 g, 1.06 mmol) in 35 mL of diethyl ether, resulting in the immediate precipitation of a brown-yellow solid. The solvent was removed by vacuum distillation and the remaining solid was dissolved in THF. After addition of $[\text{PPN}][\text{tosylate}]$ (0.79 g, 1.1 mmol), the solution was filtered through Celite and recrystallized from THF/hexane to provide a light brown product. The infrared spectrum in the $\nu(\text{CO})$ region in THF: 2039 (w), 1895 (s), 1863 (m).

Kinetic Measurements of Carbon Dioxide or Carbon Monoxide Insertion Processes. When elevated pressures were not required, these reactions were performed in a 100-mL Schlenk flask. In a typical experiment the reaction vessel was charged with the solid sample and evacuated under vacuum. Dry degassed solvent was added by cannula or syringe (solution concentration ca. 5×10^{-3} M), and the flask was backfilled with carbon dioxide or carbon monoxide at atmospheric pressure. The reaction solution was maintained at constant temperature by a thermostated water bath. Samples were withdrawn at various intervals by syringe and the reactions were monitored by infrared spectroscopy, using the IBM FTIR/85 instrument, in the $\nu(\text{CO})$ region. The progress of the reaction was followed by monitoring the disappearance of a strong,

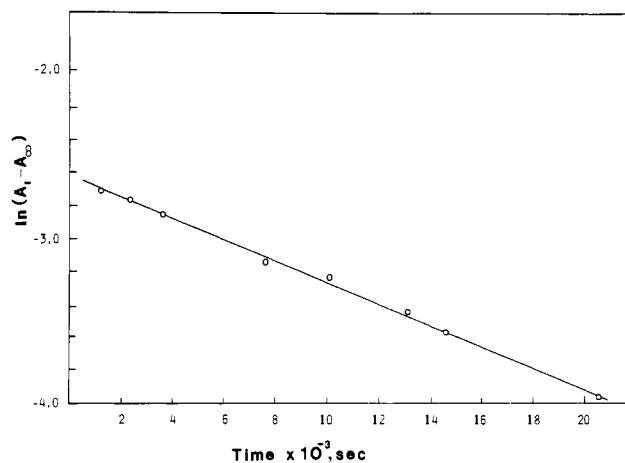


Figure 1. Pseudo-first-order plot for the reaction of $[\text{PPN}][\text{cis-CH}_3\text{W}(\text{CO})_4\text{P}(\text{OMe})_3]$ with CO_2 (760 torr) in tetrahydrofuran at 25 °C.

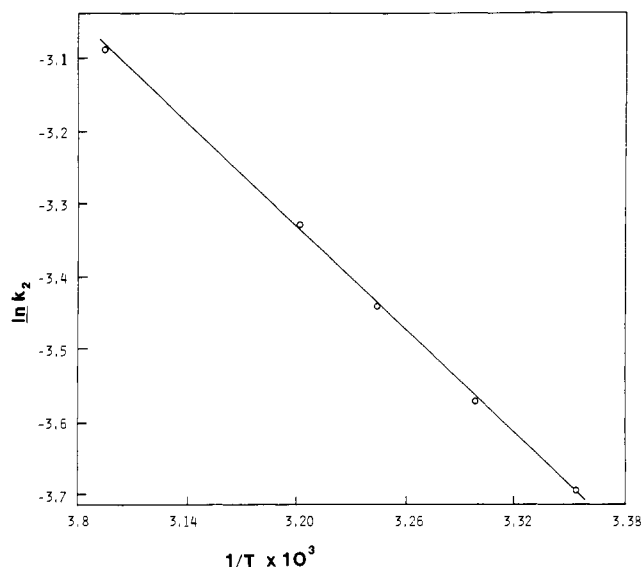


Figure 2. Arrhenius plot for the reaction of $[\text{PPN}][\text{cis-CH}_3\text{W}(\text{CO})_4\text{P}(\text{OMe})_3]$ with CO_2 (760 torr).

isolated band in the starting material. The temperature-dependent solubility data for CO_2 in tetrahydrofuran at 760 torr were obtained from extrapolation of published data.²¹ Representative rate data obtained specifically for the insertion of carbon dioxide into $[\text{PPN}][\text{cis-W}(\text{CO})_4\text{P}(\text{OMe})_3]\text{CH}_3$ at atmospheric pressure in a large excess of CO_2 (i.e., under pseudo-first-order conditions) are depicted graphically in Figures 1 and 2.

Those reactions which required higher pressures were performed in a 300-mL Parr reactor. The stainless steel reactor was evacuated and the metal complex solution prepared under nitrogen was transferred through a cannula. The system was then pressurized with carbon dioxide or carbon monoxide to the desired pressure and stirred at ambient temperature. Temperatures other than ambient were maintained by immersing the reactor in a constant temperature water bath. Samples were withdrawn by means of a dip tube at regular time intervals into capped vials. These solutions were immediately analyzed by infrared spectroscopy in the $\nu(\text{CO})$ region as described above.

Infrared Band-Shape Analysis. Infrared band shapes of the carbonyl stretching vibrations in solutions containing mixtures of metal carbonyl derivatives having grossly overlapped bands were calculated. The analyses were carried out in our laboratories using a program based on the work of R. N. Jones and J. Pitha of the

(19) Maher, J. M.; Beatty, R. P.; Cooper, N. J. *Organometallics* **1982**, *1*, 215.

(20) (a) Cotton, F. A.; Darensbourg, D. J.; Kolthammer, B. W. S. *J. Am. Chem. Soc.* **1981**, *103*, 398. (b) Cotton, F. A.; Darensbourg, D. J.; Kolthammer, B. W. S. *Inorg. Chem.* **1982**, *21*, 1656.

(21) The concentration of CO_2 in tetrahydrofuran at 25 °C and 760 torr is ca. 0.332 M. This datum and other CO_2 solubility data as a function of temperature were taken from the following: Endre, B.; Bor, G.; Marta, M. S.; Gabor, M.; Bela, M.; Geza, S. *Veszpremi Vegyip. Egy. Kozl.* **1957**, *1*, 89.

Division of Pure Chemistry, National Research Council of Canada.²² The program, modified for our use, fits a Cauchy-Gauss product and/or sum function to an infrared absorption band envelope. It has been described in detail elsewhere.²³ Spectral data points were taken every 0.96 cm⁻¹ from the Aspect 2000 computer of the IBM FTIR/85 system and inputted directly into a VAX 11/780 computer for band-shape analysis.

X-ray Crystallographic Study of [PPN][*cis*-CH₃W-(CO)₄PMe₃].²⁴ Data Collection and Reduction. A yellow prismatic crystal of C₄₄H₄₂NO₄P₃W having dimensions of 0.10 × 0.20 × 0.30 mm was mounted on a glass fiber with its long axis roughly parallel to the ϕ axis of the goniometer. The crystal was immediately cooled to low temperature on the diffractometer. Preliminary examination and data collection were performed with Mo K α radiation ($\lambda = 0.71073$ Å) on an Enraf-Nonius CAD4 computer controlled K axis diffractometer equipped with a graphite crystal, incident beam monochromator.

Cell constants and an orientation matrix for data collection were obtained from least-squares refinement, using the setting angles of 25 reflections in the range $4 < \theta < 17^\circ$, measured by the computer controlled diagonal slit method of centering. As a check on crystal quality, ω - 2θ scans of several intense reflections were measured; the width at half-height was 0.20° with a take-off angle of 2.8°, indicating good crystal quality. From the systematic absences of hkl $h + k = 2n + 1$, $h0l$ $h = 2n + 1$ ($l = 2n + 1$) and from subsequent least-squares refinement, the space group was determined to be *Cc* (No. 9).

The data were collected at a temperature of -99 ± 1 °C with the ω - 2θ scan technique. A total of 5311 reflections were collected, of which 4954 were unique and not systematically absent. As a check on crystal and electronic stability three representative reflections were measured every 41 min. The intensities of these standards remained constant within experimental error throughout data collection. No decay correction was applied.

Structure Solution and Refinement. The structure was solved by using the Patterson heavy-atom method which revealed the position of the W atom. The remaining atoms were located in succeeding difference Fourier syntheses. Hydrogens were included in calculated positions (assuming idealized geometries with C-H = 0.95 Å) and were not refined. A difference Fourier map indicated that the tungsten methyl group hydrogens (which would have been labeled H1, H2, and H3) were rotationally disordered and they were not included in the calculations. The structure was refined in full-matrix least squares where the function minimized was $\sum w(|F_o| - |F_c|)^2$ and the weight w is defined as $4F_o^2/\sigma^2(F_o^2)$.

Scattering factors were taken from Cromer and Waber.²⁵ Anomalous dispersion effects were included in F_c .²⁶ The values for $\Delta f'$ and $\Delta f''$ were those of Cromer.²⁷ Only the 4034 reflections having intensities greater than 3.0 times their standard deviation were used in the refinements. The final cycle of refinement included 476 variable parameters and converged (largest parameter shift was 0.10 times its esd) with unweighted and weighted agreement factors of 0.0357 and 0.0435, respectively. The standard deviation of an observation of unit weight was 0.99. Refinement of the other enantiomer yielded significantly higher residuals ($R_1 = 0.0374$ and $R_2 = 0.0464$). All results reported herein refer to the enantiomer which yielded the lower R values. The highest peak in the final difference Fourier had a height of 0.89 e/Å³ with an estimated error based on ΔF ²⁸ of 0.11. Plots of $\sum w(|F_o| - |F_c|)^2$ vs. $|F_o|$, reflection order in data collection, \sin

Table II. Crystallographic Summary

A. Crystal Data	
formula	C ₄₄ H ₄₂ NO ₄ P ₃ W
fw	925.60
cryst dims, mm	0.10 × 0.20 × 0.30
space group	<i>Cc</i>
lattice constants	
<i>a</i> , Å	16.538 (8)
<i>b</i> , Å	17.102 (9)
<i>c</i> , Å	16.106 (7)
β , deg	115.26 (3)
<i>V</i> , Å ³	4119.7
<i>Z</i>	4
P_{calcd} , g/cm ³	1.49
B. Intensity Measurements	
instrument	Enraf-Nonius CAD4 diffractometer
radiation	graphite monochromated Mo K α ($\lambda = 0.71073$ Å)
scan type	ω - θ
scan rate, deg/min	3–20 deg/min (in ω)
scan width, deg	$0.8 \pm 0.350 \tan \theta$
max 2θ , deg	56.0
no. of reflctns measd	5311 total, 4954 unique
corrcctns	Lorentz-polarization empirical absorption (from 0.78 to 1.00)
μ , cm ⁻¹	3/0.3
C. Structure Solution and Refinement	
solutn	Patterson method
hydrogen atoms	included in calcd positions
refinement	full-matrix least squares
minimization function	$\sum w(F_o - F_c)^2$
least-squares weights	$4F_o^2/\sigma^2(F_o^2)$
"ignorance" factor	0.060
anomalous dispersion	all non-hydrogen atoms
reflctns included	4034 with $F_o^2 > 3.0\sigma(F_o^2)$
parameters refined	476
unweighted agreement factor ^a	0.036
weighted agreement factor ^b	0.043
esd of observn of unit weight	0.99
convergence	
largest shift	0.10 σ
high peak in final diff map, e/Å ³	0.89 (11)

$$^a R_1 = \sum ||F_o| - |F_c|| / \sum |F_o|. \quad ^b R_2 = [\sum w(|F_o| - |F_c|)^2 / \sum w F_o^2]^{1/2}.$$

θ/λ , and various classes of indices showed no unusual trends.

All calculations were performed on a PDP-11/60 based TEXRAY²⁹ system, which includes the Enraf-Nonius SDP and proprietary crystallographic software of Molecular Structure Corp. Table II contains a summary of crystallographic data and analysis. Final positional and thermal parameters are given in Table III.

Tables listing observed and calculated structure factors are available as supplementary material.

Synthesis of Anionic Metal Carbonyl-Alkyls and Aryls. Two synthetic routes to group 6B RM(CO)₅⁻ compounds have previously been reported. Ellis and Hagen prepared these derivatives where M = Cr, W and R = CH₃, C₂H₅, CH₂C₆H₅, and CH₂CN via alkylation of Na₂M(CO)₅ (obtained from sodium metal reduction of M(CO)₆ in liquid ammonia or DME) with alkyl halides.¹⁷ Whereas Casey and Polichnowski synthesized the alkylammonia salts of RW(CO)₅⁻ (R = CH₃, C₆H₅, C₆H₄-*m*-CH₃, C₆H₄-*p*-CH₃, and CH₂C₆H₅) from W(CO)₅Cl⁻ and the corresponding alkyl- or aryllithium reagent.¹⁵ Alternatively, these latter researchers examined the production of RW(CO)₅⁻ derivatives by photochemical extrusion of CO in the RC(O)W(CO)₅⁻ species.



In this report we have utilized both procedures with some slight modifications, these being an alternative preparation of the Na₂M(CO)₅ salts using Cooper's labile ligand approach¹⁹ and

(22) Jones, R. N.; Pitha, J. Bulletin No. 12, National Research Council of Canada, 1968, and references therein.

(23) Hyde, C. L.; Darensbourg, D. J. *Inorg. Chem.* **1973**, *12*, 1075.

(24) These services were performed by the crystallographic staff of Molecular Structure Corp.: Dr. M. W. Extine, Ms. R. A. Meisner, Dr. J. M. Troup, and Ms. B. B. Warrington.

(25) Cromer, D. T.; Waber, J. T. "International Tables for X-ray Crystallography"; Kynoch Press: Birmingham, England, 1974; Vol. IV, Table 2.2B.

(26) Ibers, J. A.; Hamilton, W. C. *Acta Crystallogr.* **1964**, *17*, 781.

(27) Cromer, D. T. "International Tables for X-ray Crystallography"; Kynoch Press: Birmingham, England, 1974; Vol. IV, Table 2.3.1.

(28) Cruikshank, D. W. J. *Acta Crystallogr.* **1949**, *2*, 154.

(29) TEXRAY is a trademark of Molecular Structure Corp. (1982).

Table III. Table of Positional and Thermal Parameters and Their Estimated Standard Deviations^a

atom	x	y	z	$\beta(1,1)$	$\beta(2,2)$	$\beta(3,3)$	$\beta(1,2)$	$\beta(1,3)$	$\beta(2,3)$
W1	0.0000	0.20628 (2)	0.0000	0.00365 (1)	0.00192 (1)	0.00299 (1)	-0.00048 (3)	0.00325 (1)	-0.00073 (3)
P1	0.1163 (2)	0.3013 (1)	0.1047 (2)	0.00483 (9)	0.00228 (8)	0.00398 (9)	-0.0003 (1)	0.00377 (13)	-0.0013 (1)
P2	0.4137 (1)	0.6731 (1)	0.4354 (1)	0.00276 (6)	0.00149 (5)	0.00175 (6)	0.0011 (1)	0.00151 (9)	0.001 (1)
P3	0.4122 (1)	0.8480 (1)	0.4188 (1)	0.00204 (6)	0.00153 (5)	0.00217 (6)	0.0002 (1)	0.00156 (9)	0.0001 (1)
O1	-0.1444 (5)	0.0912 (4)	-0.1316 (5)	0.0059 (3)	0.0032 (3)	0.0052 (3)	-0.0021 (5)	0.0048 (4)	0.0003 (5)
O2	0.1126 (6)	0.0690 (5)	0.1337 (5)	0.0093 (5)	0.0033 (3)	0.0046 (3)	0.0013 (7)	0.0022 (7)	0.0015 (6)
O3	0.1278 (5)	0.1845 (6)	-0.0995 (6)	0.0074 (3)	0.0059 (4)	0.0088 (4)	-0.0041 (6)	0.0114 (4)	-0.0038 (6)
O4	-0.0957 (8)	0.3456 (6)	-0.1339 (7)	0.0127 (7)	0.0041 (4)	0.0081 (5)	0.0016 (9)	0.0043 (10)	0.0042 (8)
N1	0.4351 (4)	0.7629 (4)	0.4586 (4)	0.0028 (2)	0.0019 (2)	0.0027 (2)	0.0006 (4)	0.0021 (3)	-0.0005 (4)
C1	-0.0887 (5)	0.1346 (5)	-0.0829 (6)	0.0037 (3)	0.0022 (3)	0.0041 (3)	-0.0003 (5)	0.0037 (4)	0.0020 (5)
C2	0.0690 (7)	0.1200 (5)	0.0850 (6)	0.0067 (5)	0.0020 (3)	0.0030 (3)	-0.0012 (6)	0.0032 (6)	-0.0009 (5)
C3	0.0851 (8)	0.1943 (6)	-0.0652 (6)	0.0078 (5)	0.0036 (4)	0.0037 (3)	0.0018 (7)	0.0058 (6)	-0.0004 (6)
C4	-0.0612 (9)	0.2954 (6)	-0.0848 (9)	0.0066 (6)	0.0025 (3)	0.0065 (6)	0.0002 (8)	0.0026 (10)	-0.0010 (8)
C5	-0.0793 (10)	0.2227 (11)	0.0775 (13)	0.0047 (6)	0.0091 (9)	0.0127 (10)	0.0005 (12)	0.0047 (12)	0.0094 (14)
C6	0.0915 (10)	0.3498 (9)	0.1904 (11)	0.0086 (7)	0.0060 (6)	0.0123 (8)	-0.0022 (11)	0.0104 (10)	-0.0098 (10)
C7	0.1434 (12)	0.3796 (9)	0.0527 (11)	0.0142 (11)	0.0052 (6)	0.0071 (7)	-0.0087 (13)	0.0050 (15)	-0.0032 (12)
C8	0.2256 (10)	0.2622 (11)	0.1739 (12)	0.0053 (6)	0.0063 (6)	0.0112 (10)	-0.0017 (12)	0.0017 (14)	-0.0060 (14)
C9	0.4138 (5)	0.6271 (5)	0.5360 (4)	0.0029 (3)	0.0021 (2)	0.0020 (2)	0.0007 (5)	0.0016 (4)	0.0009 (4)
C10	0.4423 (6)	0.6675 (5)	0.6185 (5)	0.0039 (3)	0.0024 (3)	0.0027 (3)	0.0009 (6)	0.0017 (5)	0.0001 (5)
C11	0.4421 (6)	0.6320 (6)	0.6956 (5)	0.0048 (4)	0.0043 (4)	0.0012 (2)	0.0002 (7)	0.0023 (4)	0.0002 (5)
C12	0.4134 (6)	0.5562 (6)	0.6906 (6)	0.0050 (4)	0.0037 (4)	0.0038 (3)	0.0008 (6)	0.0044 (5)	0.0031 (6)
C13	0.3861 (6)	0.5148 (6)	0.6117 (6)	0.0053 (3)	0.0032 (3)	0.0045 (3)	-0.0006 (6)	0.0062 (4)	0.0021 (6)
C14	0.3849 (5)	0.5505 (5)	0.5332 (5)	0.0038 (3)	0.0026 (3)	0.0035 (3)	0.0003 (5)	0.0039 (4)	0.0005 (5)
C15	0.4981 (5)	0.6277 (5)	0.4078 (4)	0.0031 (3)	0.0019 (2)	0.0022 (2)	0.0017 (4)	0.0021 (4)	0.0002 (4)
C16	0.5328 (7)	0.6699 (6)	0.3577 (7)	0.0102 (4)	0.0035 (3)	0.0088 (4)	0.0080 (6)	0.0155 (5)	0.0062 (6)
C17	0.5963 (7)	0.6387 (8)	0.3328 (7)	0.0120 (4)	0.0051 (5)	0.0141 (4)	0.0064 (7)	0.0239 (5)	0.0060 (8)
C18	0.6265 (7)	0.5644 (7)	0.3599 (7)	0.0076 (4)	0.0042 (4)	0.0069 (4)	0.0051 (7)	0.0098 (6)	0.0006 (7)
C19	0.5956 (6)	0.5221 (5)	0.4118 (6)	0.0048 (3)	0.0021 (3)	0.0049 (4)	0.0033 (5)	0.0047 (5)	0.0015 (6)
C20	0.5295 (5)	0.5534 (5)	0.4355 (6)	0.0035 (3)	0.0019 (3)	0.0045 (3)	0.0016 (5)	0.0033 (5)	0.0003 (5)
C21	0.3073 (5)	0.6532 (4)	0.3432 (4)	0.0033 (3)	0.0015 (2)	0.0018 (2)	0.0002 (4)	0.0015 (4)	-0.0002 (4)
C22	0.2313 (5)	0.6860 (5)	0.3457 (6)	0.0034 (3)	0.0023 (3)	0.0044 (3)	0.0000 (5)	0.0046 (4)	0.0001 (5)
C23	0.1446 (6)	0.6719 (6)	0.2707 (6)	0.0030 (3)	0.0032 (3)	0.0035 (3)	-0.0007 (6)	0.0019 (5)	0.0010 (6)
C24	0.1375 (6)	0.6249 (6)	0.2014 (6)	0.0032 (4)	0.0032 (3)	0.0033 (4)	-0.0029 (6)	-0.0012 (6)	-0.0012 (6)
C25	0.2143 (7)	0.5924 (7)	0.1992 (6)	0.0060 (5)	0.0036 (4)	0.0019 (3)	0.0002 (8)	-0.0001 (6)	-0.0005 (5)
C26	0.2991 (6)	0.6058 (5)	0.2704 (5)	0.0038 (3)	0.0029 (3)	0.0019 (3)	0.0033 (5)	-0.0006 (5)	-0.0005 (5)
C27	0.3196 (5)	0.8547 (4)	0.3074 (5)	0.0019 (2)	0.0018 (2)	0.0023 (3)	0.0011 (4)	0.0000 (4)	0.0006 (5)
C28	0.3259 (5)	0.8180 (5)	0.2342 (5)	0.0026 (3)	0.0023 (3)	0.0029 (3)	-0.0003 (5)	0.0009 (5)	0.0012 (5)
C29	0.2521 (7)	0.8139 (6)	0.1519 (5)	0.0061 (5)	0.0028 (3)	0.0013 (3)	-0.0011 (6)	0.0016 (5)	-0.0001 (5)
C30	0.1705 (6)	0.8495 (6)	0.1385 (7)	0.0032 (4)	0.0041 (4)	0.0044 (4)	0.0024 (7)	0.0001 (7)	0.0035 (7)
C31	0.1642 (5)	0.8884 (6)	0.2112 (7)	0.0021 (3)	0.0040 (4)	0.0051 (4)	0.0030 (6)	0.0012 (6)	0.0008 (7)
C32	0.2379 (5)	0.8898 (5)	0.2951 (6)	0.0028 (3)	0.0015 (2)	0.0047 (4)	0.0019 (5)	0.0022 (5)	0.0013 (5)
C33	0.5064 (5)	0.8917 (6)	0.4066 (5)	0.0023 (2)	0.0036 (3)	0.0031 (3)	-0.0019 (5)	0.0027 (4)	-0.0014 (5)
C34	0.5924 (5)	0.8612 (7)	0.4565 (6)	0.0024 (3)	0.0055 (5)	0.0039 (3)	-0.0003 (6)	0.0032 (4)	-0.0027 (9)
C35	0.6632 (5)	0.8943 (9)	0.4465 (7)	0.0020 (3)	0.0085 (7)	0.0054 (4)	-0.0003 (8)	0.0034 (5)	-0.0027 (9)
C36	0.6503 (6)	0.9602 (8)	0.3907 (7)	0.0059 (4)	0.0086 (6)	0.0059 (4)	-0.0104 (7)	0.0067 (6)	-0.0056 (9)
C37	0.5656 (7)	0.9902 (8)	0.3425 (7)	0.0064 (4)	0.0060 (5)	0.0057 (5)	-0.0057 (8)	0.0060 (6)	0.0003 (8)
C38	0.4928 (6)	0.9565 (6)	0.3494 (6)	0.0046 (3)	0.0034 (3)	0.0053 (4)	-0.0023 (6)	0.0053 (5)	0.0011 (6)
C39	0.3863 (5)	0.9077 (4)	0.4958 (5)	0.0027 (3)	0.0015 (2)	0.0024 (3)	0.0008 (4)	0.0010 (4)	-0.0005 (4)
C40	0.3565 (7)	0.8731 (7)	0.5532 (6)	0.0070 (4)	0.0035 (4)	0.0055 (4)	0.0008 (7)	0.0079 (5)	-0.0020 (6)
C41	0.3303 (7)	0.9185 (8)	0.6105 (7)	0.0101 (5)	0.0059 (6)	0.0074 (4)	0.0048 (9)	0.0137 (5)	0.0010 (8)
C42	0.3343 (7)	0.9986 (7)	0.6071 (7)	0.0057 (5)	0.0045 (4)	0.0046 (4)	0.0046 (7)	0.0017 (7)	-0.0041 (6)
C43	0.3637 (8)	1.0348 (6)	0.5479 (8)	0.0084 (6)	0.0022 (3)	0.0064 (5)	0.0014 (7)	0.0046 (9)	-0.0034 (7)
C44	0.3918 (7)	0.9897 (6)	0.4939 (7)	0.0063 (5)	0.0023 (3)	0.0057 (4)	0.0003 (7)	0.0052 (7)	-0.0018 (6)

^aThe form of the anisotropic thermal parameter is as follows: $\exp[-(\beta(1,1)h^2 + \beta(2,2)k^2 + \beta(3,3)l^2 + \beta(1,2)hk + \beta(1,3)hl + \beta(2,3)kl)]$. Estimated standard deviations in the least significant digits are shown in parentheses.

alkylations in general being accomplished with alkyl tosylates in order to avoid the introduction of halide ion in the metal's coordination sphere. In addition, metathesis of the sodium salts with [PPN][tosylate] further avoided metal-chloride impurities (this is especially the case for *cis*-R²W(CO)₄PR₃⁻ derivatives).

Because of the sensitivity of the kinetic parameters to alkali metal ions for CO₂ insertion reactions involving RM(CO)₅⁻ species, it was extremely important to remove these contaminants prior to rate measurements.^{7,8,30} This was accomplished by repeated washing of the samples with deoxygenated water. These complexes are stable toward hydrolysis because of their insolubility in water. By way of contrast, the CH₃W(CO)₅⁻ derivative undergoes rapid reaction upon dissolution in methanol to yield CH₄ and CH₃O-W(CO)₅⁻, with subsequent reactions affording (CH₃OH)W(CO)₅.^{31,32}

All alkyl- and aryltungsten pentacarbonyl derivatives were quite stable in organic solvents, e.g., THF or acetonitrile, for extended periods of time (days) under anaerobic conditions. In particular the ethyl derivative, which is capable of β -hydrogen elimination with metal-hydride production, is quite inert in THF at ambient temperature. However, upon refluxing this alkyl complex in THF (~66 °C) the C₂H₅C(O)W(CO)₅⁻ derivative is produced. This is to be contrasted with the methyl analogue where higher temperature (refluxing DME, ~83 °C) are required to influence carbonylation (vide infra). Photoinduced β -hydrogen transfer occurs upon photolysis of C₂H₅W(CO)₅⁻ at ambient temperature, with μ -H[W(CO)₅]₂⁻ being the ultimate metal containing species produced.³³

The W(CO)₅R⁻ species display solution spectroscopic properties expected for metal pentacarbonyl derivatives. Three infrared

(30) Darensbourg, D. J.; Pala, M. *J. Am. Chem. Soc.* **1985**, *107*, 5687.

(31) Darensbourg, D. J.; Gray, R. L.; Ovalles, C.; Pala, M. *J. Mol. Catal.* **1985**, *29*, 285.

(32) Unpublished results from our laboratories.

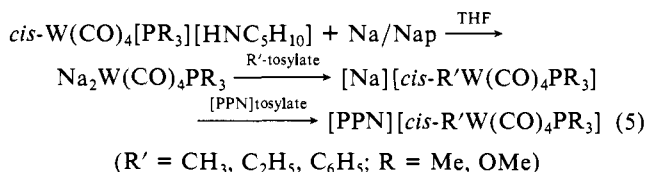
(33) For an excellent review of these type of processes see: Alt, H. G. *Angew. Chem., Int. Ed. Engl.* **1984**, *23*, 766.

Table IV. Bond Lengths (Å) and Angles (deg) for the Anion *cis*-CH₃W(CO)₄P(CH₃)₃⁻

bond lengths (Å)			bond angles (deg)							
atom 1	atom 2	distance (Å)	atom 1	atom 2	atom 3	angle (deg)	atom 1	atom 2	atom 3	angle (deg)
W1	P1	2.532 (3)	P1	W1	C1	178.5 (4)	C3	W1	C5	175 (1)
W1	C1	1.941 (13)	P1	W1	C2	88.2 (4)	C4	W1	C5	92.3 (8)
W1	C2	2.005 (13)	P1	W1	C3	85.1 (5)	W1	P1	C6	116.7 (6)
W1	C3	2.09 (2)	P1	W1	C4	89.1 (4)	W1	P1	C7	116.9 (6)
W1	C4	2.008 (15)	P1	W1	C5	90.4 (7)	W1	P1	C8	116.8 (6)
W1	C5	2.18 (3)	C1	W1	C2	92.8 (4)	C6	P1	C7	102 (1)
P1	C6	1.80 (2)	C1	W1	C3	93.8 (6)	C6	P1	C8	101.1 (9)
P1	C7	1.74 (2)	C1	W1	C4	89.9 (6)	C7	P1	C8	101 (1)
P1	C8	1.80 (2)	C1	W1	C5	90.7 (8)	W1	C1	O1	178 (1)
O1	C1	1.183 (15)	C2	W1	C3	87.8 (6)	W1	C2	O2	177 (1)
O2	C2	1.19 (2)	C2	W1	C4	176.1 (7)	W1	C3	O3	177 (1)
O3	C3	1.08 (2)	C2	W1	C5	90.6 (7)	W1	C4	O4	179 (2)
O4	C4	1.14 (2)	C3	W1	C4	89.1 (7)				

bands in the $\nu(\text{CO})$ region are observed (Table I) of intensity pattern weak ($A_1^{(2)}$), strong (E), and medium ($A_1^{(1)}$), with a weak forbidden B_1 band also being noted.³⁴ This $\nu(\text{CO})$ infrared intensity pattern and peak positions are not affected by excess Na^+ ions, as revealed by the addition of NaBPh_4 to THF solutions of $\text{CH}_3\text{W}(\text{CO})_5^-$. The ^{13}C NMR exhibits two peaks in the carbonyl region, e.g., for $\text{CH}_3\text{W}(\text{CO})_5^-$ in THF at 208.1 and 207.5 ppm, of intensity ratio ca. 1:4.

The *cis*- $\text{W}(\text{CO})_4[\text{PR}_3]\text{Cl}^-$ derivatives were found to be unreactive toward methyl lithium,³⁵ hence the synthesis of phosphine substituted alkyl or aryl complexes was accomplished by alkylation of the tetracarbonyl-phosphine or -phosphite metallates with alkyl- or aryl-tosylates (eq 5). Alkylation with alkyl halides resulted in production of large quantities of the phosphine/phosphite substituted metal halide derivatives. Similarly, sizable amounts of the *cis*- $\text{W}(\text{CO})_4[\text{PR}_3]\text{Cl}^-$ anions were observed when the once prepared $[\text{Na}][\text{cis-R}'\text{W}(\text{CO})_4\text{PR}_3]$ salts were cation exchanged with $[\text{PPN}]\text{Cl}$, hence $[\text{PPN}]\text{tosylate}$ was employed in the methathesis reaction.³⁶



The infrared spectra in the $\nu(\text{CO})$ region of these $[\text{cis-R}'\text{W}(\text{CO})_4\text{PR}_3][\text{PPN}]$ salts dissolved in THF solution consist of three peaks of intensity pattern weak (A'), strong ($A' + A''$), and medium (A'), with the strong peak displaying a shoulder at high frequency. These spectra are quite similar to those previously reported for the analogous hydride derivatives, $[\text{PPN}][\text{cis-HW}(\text{CO})_4\text{PR}_3]$.¹⁸ The *cis*- $\text{R}'\text{W}(\text{CO})_4\text{PR}_3^-$ anions were observed to form contact ion pairs with Na^+ ions in THF solution. In addition to peaks corresponding to the symmetric anion, a peak assignable to Na^+ interaction at a CO site ($\nu(\text{CO})$ shift to lower frequency) was noted with a concomitant shifting of the remaining $\nu(\text{CO})$ vibrations to higher frequencies.³⁷ The specific CO site of alkali metal ion pairing is presumably the carbonyl ligand trans to the PR_3 ligand since this CO group is involved in π -back-bonding with the metal center to the greatest extent (*vide infra*).³⁸ This observation is to be contrasted with alkali metal ion pairing with the *cis*- $\text{HW}(\text{CO})_4\text{PR}_3^-$ anions where alkali metal ion interaction occurs at the hydride site.³⁹

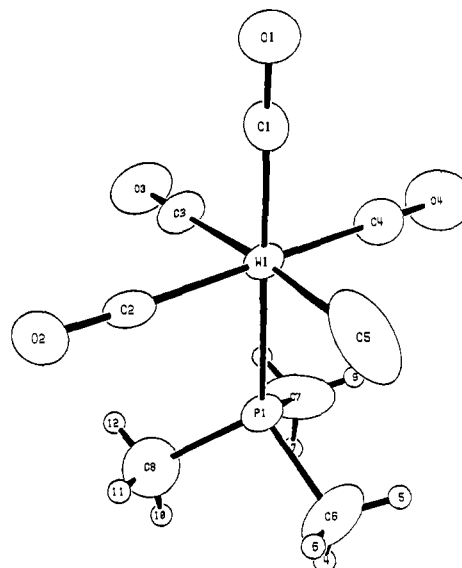
(34) Restricted CO stretching force field computations for $\text{CH}_3\text{W}(\text{CO})_5^-$ in THF yield $k_1 = 13.76$, $k_2 = 15.03$, and $k_i = 0.353$, with a predicted B_1 band at 1929 cm^{-1} .

(35) The reactivity of *cis*- $\text{W}(\text{CO})_4[\text{PR}_3]\text{Cl}^-$ with methyl lithium can be enhanced in the presence of TMEDA. Personal communications with Professor W. Schenk (Würzburg).

(36) Presently, we do not understand this seemingly carbanion substitution reaction.

(37) Darensbourg, M. Y. *Prog. Inorg. Chem.* **1985**, *33*, 221 and references therein.

(38) A detailed analysis of the solution structures of these $[\text{Na}][\text{cis-R}'\text{W}(\text{CO})_4\text{PR}_3]$ salts by infrared spectroscopy is currently in progress.

**Figure 3.** ORTEP drawing of the *cis*-CH₃W(CO)₄PMe₃⁻ anion.

Molecular Structure of $[\text{PPN}][\text{cis-CH}_3\text{W}(\text{CO})_4\text{P}(\text{CH}_3)_3]$. The solid-state structure of $[\text{PPN}][\text{cis-CH}_3\text{W}(\text{CO})_4\text{PMe}_3]$ has been determined at -99°C and provides the first (alkyl)C-W bond distance in a zero-valent tungsten complex. The final atomic coordinates and thermal parameters are collected in Table III. Interatomic distances and angles for the anion are provided in Table IV, whereas, those for the ubiquitous PPN^+ cation may be found in the supplementary material. A view of the anion is depicted in Figure 3, where the atomic numbering scheme is defined as well.

The arrangement of the ligands around the central tungsten atom closely defines a regular octahedron. The longest coordination sphere bond, W-P(1), has a length of 2.532 (3) Å while the W-C(5) bond distance is 2.18 (3) Å. This W-P distance is quite similar to those noted in the closely related anion, *cis*- $\text{CH}_3\text{CO}_2\text{W}(\text{CO})_4\text{PEt}_3^-$,⁴⁷ and the neutral complex $\text{W}(\text{CO})_5\text{PMe}_3$,⁴⁰ where metal-phosphorus distances of 2.533 (5) and 2.516 (2) Å were observed. On the other hand, the sterically encumbered $\text{W-P}(t\text{-Bu})_3$ grouping displays a W-P bond length much longer, 2.686 (4) Å.⁴¹ The W-CH₃ bond distance of 2.18 (3) Å is somewhat shorter than that seen in the isoelectronic neutral Re-CH_3 analogue, where a bond distance of 2.308 (17) Å has been reported.⁴² There are meaningful differences among the W-CO bond distances, in particular the W-C(1) bond which

(39) Kao, S. C.; Darensbourg, M. Y.; Schenk, W. *Organometallics* **1984**, *3*, 871.

(40) Cotton, F. A.; Darensbourg, D. J.; Kolthammer, B. W. S. *Inorg. Chem.* **1981**, *20*, 4440.

(41) Pickardt, Von J.; Rösch, L.; Schumann, H. Z. *Anorg. Allg. Chem.* **1976**, *426*, 66.

(42) Rankin, D. W. H.; Robertson, A. J. *Organomet. Chem.* **1976**, *105*, 331.

Table V. Pressure Dependence on Rate of CO₂ Insertion into the W–CH₃ Bond in [PPN][W(CO)₅CH₃] Complex^a

total pressure (psi) ^b	k_{obsd} , s ⁻¹ × 10 ⁶	total pressure (psi) ^b	k_{obsd} , s ⁻¹ × 10 ⁶
14.7	1.15	200	30.5
14.7	0.832 ^c	200	37.2
50	8.33	300	69.8
100	13.8	400	133
130	25.8	500	183
150	16.2	500	217

^a Tetrahydrofuran solvent, 23 °C. ^b $P_{\text{total}} = P_{\text{CO}_2} + P_{\text{THF}}(1 - X_{\text{CO}_2})$, where P_{THF} at 23 °C = 2.8 psi. Errors in pressure measurements are approximately ±5%. ^c Corrected for decomposition of starting material, [PPN][W(CO)₅CH₃], in THF solution.

is trans to the PMe₃ ligand is somewhat shorter at 1.941 (13) Å than the mutually trans W–C(2) and W–C(4) distances of 2.005 (13) and 2.008 (15) Å, respectively. In turn these are slightly shorter than the W–C(3) bond distance of 2.09 (2) Å which is trans to the methyl group. Hence, the PMe₃ ligand exerts its expected trans M–C bond tightening, whereas the CH₃ group causes a trans M–C bond lengthening.

The angles around the tungsten atom approximate closely to the expected octahedral angles of 90° and 180°. The largest deviation from octahedral geometry was observed for the CH₃ group and its trans CO ligand, C(3)–W–C(5), where an angle of 175.1° was noted. There was no apparent steric interaction between the small phosphine ligand, PMe₃, and the methyl group with the P(1)–W–C(5) angle being 90.4 (7)°. Previously we have shown that even phosphine ligands possessing small cone angles, when situated cis to one another, can exert steric interference, e.g., the P–Mo–P angle in *cis*-Mo(CO)₄[PMe₃]₂ was found to be 97.54°. ⁴³

The trimethylphosphine ligand has normal bond distances and angles. The average P–C distance and C–P–C angle are 1.78 (2) Å and 101.4°, respectively. The PPN⁺ cation is of the ubiquitous bent variety with a P–N–P angle of 144.2 (5)°. The average P–N bond length is 1.578 (8) Å, and the conformation and positions of the phenyl rings produced standard bond distances and angles (supplementary material).

Kinetic Studies of Carbon Dioxide Insertion Reactions. Kinetic measurements of carbon dioxide insertion into the tungsten–carbon bond were carried out primarily with *cis*-CH₃W(CO)₄L⁻ (L = CO or phosphorus ligand) derivatives as substrates. Reactions were run in excess carbon dioxide, i.e., under conditions of pseudo-first-order behavior (eq 6). Table V contains the observed rate constants as a function of CO₂ partial pressure for reactions involving the CH₃W(CO)₅⁻ substrate at ambient (23 °C) temperature. The reactions were generally quite clean leading to W(CO)₅O₂CCH₃⁻ as the sole reaction product (see Figure 4). At

$$\text{rate} = k_2[\text{CH}_3\text{W}(\text{CO})_5^-][\text{CO}_2]^n = k_{\text{obsd}}[\text{CH}_3\text{W}(\text{CO})_5^-] \quad (6)$$

a low pressure of carbon dioxide where the insertion process occurs quite slowly (over days) decomposition of the product was observed. Control experiments of the decomposition of the acetato complex indeed verified its instability upon prolonged standing in solution ($t_{1/2}$ in THF at 25 °C = ~1 day), whereas CH₃W(CO)₅⁻ decomposed only slowly under these conditions ($t_{1/2}$ in THF at 25 °C = 13.4 days).

A plot of k_{obsd} vs. P_{CO_2} was linear up to ca. 200 psi of total pressure in tetrahydrofuran (Figure 5), i.e., $n = 1$ in eq 6. Beyond this pressure the concentration of CO₂ increases more rapidly with further increase in pressure. In other words, Henry's law (eq 7) is not obeyed at $P_{\text{total}} \geq 200$ psi, ^{44,45} where H is Henry's law constant

$$P_{\text{total}} = HX_{\text{CO}_2} + P_{\text{THF}}(1 - X_{\text{CO}_2}) \quad (7)$$

(43) Cotton, F. A.; Darensbourg, D. J.; Klein, S.; Kolthammer, B. W. S. *Inorg. Chem.* **1982**, *21*, 2661.

(44) Similar observations have been made for carbon dioxide solubility in CH₂Cl₂ solutions. ⁴⁵

(45) (a) Buell, D. S.; Eldridge, J. W. *J. Chem. Eng. Data* **1962**, *7*, 187. (b) Vonderheiden, F. H.; Eldridge, J. W. *Ibid.* **1963**, *8*, 20.

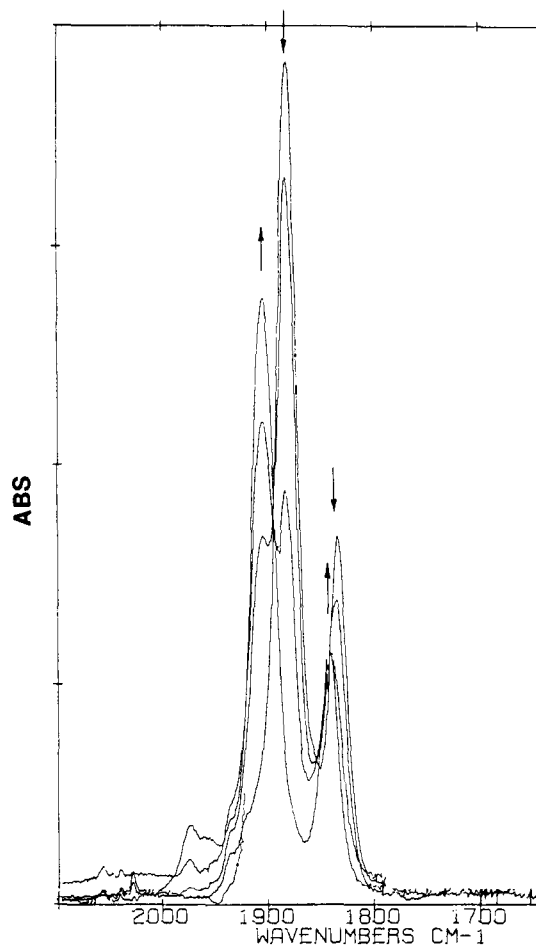
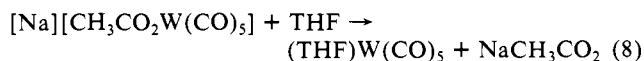


Figure 4. Representative infrared spectral traces in the $\nu(\text{CO})$ region in THF during the reaction of CH₃W(CO)₅⁻ with carbon dioxide to provide CH₃CO₂W(CO)₅⁻.

(psi), X_{CO_2} is the mole fraction of carbon dioxide in liquid phase, and P_{THF} equals 3.2 psi at 25 °C.

The insertion of carbon dioxide into the tungsten–alkyl bond of [PPN][CH₃W(CO)₅] is enhanced in the presence of an equimolar quantity of NaBPh₄ in tetrahydrofuran. For example, at 500-psi carbon dioxide pressure and ambient temperature $k_{\text{obsd}} = 11.9 \times 10^{-4}$ s⁻¹ for CO₂ insertion into [Na][CH₃W(CO)₅], compared to 2.00×10^{-4} s⁻¹ for the analogous process involving [PPN][CH₃W(CO)₅]. ³⁰ Although no Na⁺ contact ion interaction with either CH₃W(CO)₅⁻ or CO₂ in tetrahydrofuran was noted by infrared spectroscopy, the carboxylate product displays strong ion pairing between sodium ion and the distal oxygen atom of the carboxylate ligand. ³⁰ Indeed, in a reaction subsequent to the CO₂ insertion process, alkali metal assisted displacement of the carboxylate ligand by other ligands (THF or CO) readily occurs (eq 8).



Because of the deleterious effect of alkali metal ions on these anionic transition-metal carboxylates, this mode of rate enhancement is not generally useful in the conversion of CO₂ into other organic substances. That is, in reactions subsequent to the carbon-carbon bond-forming process the carboxylate ligand must remain bonded to the transition-metal species. ⁴⁶ Hence, we were interested in investigating other pathways for accelerating the reactions of carbon dioxide with transition-metal–carbon bonds. A route which might be anticipated to be effective involves reactions of carbon dioxide with a more nucleophilic metal center, for the most prominent mode of binding of CO₂ with low valence

(46) Darensbourg, D. J.; Ovalles, C. *J. Am. Chem. Soc.* **1984**, *106*, 3750.

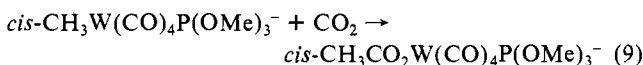
Table VI. Rate Parameters for CO₂ Insertion into the W-CH₃ Bond in [PPN][*cis*-CH₃W(CO)₄L] Complexes

L	temp, °C	[CO ₂], ^a M	k _{obsd} (s ⁻¹)	k ₂ (M ⁻¹ s ⁻¹)
P(OMe) ₃ ^b	25	0.332	6.65 × 10 ⁻⁵	2.00 × 10 ⁻⁴
	30	0.317	8.50 × 10 ⁻⁵	2.68 × 10 ⁻⁴
	35	0.302	10.9 × 10 ⁻⁵	3.63 × 10 ⁻⁴
	40	0.287	13.5 × 10 ⁻⁵	4.71 × 10 ⁻⁴
	50	0.256	21.0	8.20 × 10 ⁻⁴
PMe ₃	25	0.332	2.80 × 10 ⁻⁴	8.43 × 10 ⁻⁴

^a Extrapolated from data presented in ref 21. ^b Activation parameters: ΔH[‡] = 42.7 ± 1.0 kJ/mol, ΔS[‡] = -181.2 ± 3.8 J/mol·K, and ΔG[‡] at 25 °C = 96.7 ± 2 kJ/mol.

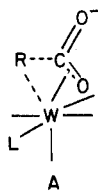
metals is in a η²-C=O fashion where CO₂ functions as a good π-acid.^{5d}

The phosphorus ligand substituted alkyl derivatives synthesized herein, where the phosphorus ligand is *sterically nonencumbering*, readily fulfill this requirement. Rate data for carbon dioxide insertion into the tungsten-methyl bond of [PPN][*cis*-CH₃W(CO)₄L] (L = PMe₃ and P(OMe)₃) are listed in Table VI. Owing to the much greater reactivity for CO₂ insertion accompanied with phosphine ligand replacement for CO, it was possible to conveniently obtain rate data at atmospheric CO₂ pressure. This is of importance since CO₂ solubility data exist for tetrahydrofuran solutions as a function of temperature at 760 mm of pressure,²¹ making it feasible to obtain activation parameters for the CO₂ insertion reaction depicted in eq 9. It is noteworthy that the products of these CO₂ insertion processes have been prepared by



CO substitution in the CH₃CO₂W(CO)₅⁻ derivative and have been fully characterized in both solution and the solid state.⁴⁷

The bimolecular rate constants (k₂) for carbon dioxide insertion into the W-CH₃ bond in *cis*-CH₃W(CO)₄L⁻ anions are shown to be significantly increased with increasing electron-donating ligands (L). That is, the rate constants (k₂) increase as a function of L, CO < P(OMe)₃ < PMe₃, with relative values of k₂ being 1:57.8:243, respectively. A similar, but less pronounced, rate enhancement has been noted for CO₂ insertion into the tungsten-alkyl bond in the W(CO)₄CH₂CH₂CH₂PPh₂⁻ derivative.⁴⁸ The activation parameters for these insertion processes (ΔH[‡] = 42.7 kJ/mol and ΔS[‡] = -181.2 J/mol·K) are indicative of an I_a mechanism involving a great deal of bond making in the transition state (A). Consistent with this interpretation, the rate for CO₂



insertion into the CH₃Cr(CO)₅⁻ species occurs ca. 6 times slower than its tungsten analogue.⁴⁹ In further support of this pathway no dissociation of CO is observed during CO₂ insertion (*vide infra*). More importantly, recent results for CO₂ insertion into *threo*-PhCHDCHDW(CO)₅⁻ and *threo*-PhCHDCHDW(CO)₄PMe₃⁻ diastereomers indicate retention of configuration at carbon.⁵⁰

Unlike migratory carbon monoxide insertion reactions involving RW(CO)₅⁻ (*vide infra*) or RMn(CO)₅,^{3,4} these carbon dioxide

Table VII. Rate Parameters for CO₂ Insertion into the W-R Bond in [PPN][RW(CO)₅] Complexes

R	k _{obsd} (s ⁻¹) ^a	relative rates
C ₆ H ₅	2.20 × 10 ⁻⁵	1.0
C ₂ H ₅	5.33 × 10 ⁻⁵ ^b	
	8.35 × 10 ⁻⁵	3.8
CH ₃	13.3 × 10 ⁻⁵	6.0

^a Temperature, 25 °C; CO₂ pressure, 400 psi; solvent, tetrahydrofuran. ^b CO₂ pressure, 300 psi.

Table VIII. Rate Parameters for Carbon Monoxide Insertion into RW(CO)₅⁻ Derivatives^a

R	k ₁ , s ⁻¹	relative rates
Ph	5.0 × 10 ⁻⁶ (400 psi)	1.0
Me	4.5 × 10 ⁻⁵ (400 psi) ^b	9.0
	5.2 × 10 ⁻⁵ (500 psi)	
Et	3.3 × 10 ⁻⁴ (14.7 psi) ^c	1000
	>5 × 10 ⁻³ (100 psi)	

^a Reactions carried out in tetrahydrofuran at ambient temperature.

^b In the presence of 1 equiv of NaBPh₄ the reaction rate for methyl migration is enhanced to 3.0 × 10⁻⁴ s⁻¹ at 400 psi of carbon monoxide.

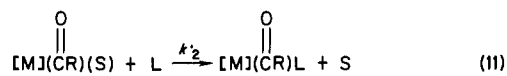
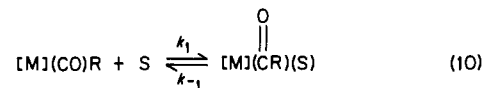
^c This value represents k_{obsd} with a mixed-order CO dependence, i.e., not the limiting value, k₁.

reactions do not exhibit a large rate dependence on the nature of the R group for R = CH₃, Et, and Ph. Table VII provides k_{obsd} values for CO₂ insertion into [PPN][RW(CO)₅] species at ambient temperature and P_{CO₂} = 400 psi. As is readily seen, the rates vary only over a factor of about 6 for the R groups investigated.

Kinetic Studies of Carbon Monoxide Insertion Reactions.

Carbon monoxide migratory insertion into the M-R bond of manganese and iron derivative displays a significant rate decrease with decreasing electron-donating ability of the R group, i.e., Et > Me > Ph.⁴ The rates of migratory CO insertion into the metal-carbon bond of RMn(CO)₅ and RFe(CO)₄⁻ correlate with Taft σ* parameters providing quite similar reaction constants ρ* of -8.8 and -8.7, respectively. These very large negative ρ* values dramatically illustrate the effect of electron-withdrawing R group in retarding the migration process, e.g., in RMn(CO)₅ R = ethyl inserts CO 10 times faster than R = Me which in turn is ca. an order of magnitude faster than R = Ph.^{3c,4} Casey and Polichnowski have similarly observed in RW(CO)₅⁻ that the phenyl derivative undergoes CO insertion approximately an order of magnitude times slower than the methyl analogue.

Kinetic investigations for migratory carbon monoxide insertion processes entailing a variety of metal substrates are consistent with the following mechanistic scheme, where S = solvent molecule.



$$\text{rate} = \frac{k_1 k_2 [M(CO)R][S][L]}{k_{-1} + k_2 [L]} = k_{\text{obsd}} [M(CO)R]$$

For the incoming ligand (L) equals CO, the reaction displays mixed order kinetics at low P_{CO} and becomes independent of P_{CO} at high pressures of carbon monoxide. Wax and Bergman have shown that the scheme above holds for (η⁵-C₅H₅)Mo(CO)₃Me as substrate with L = PMePh₂.⁵¹ The rate constant k₁ was found to decrease with the steric bulk of substituted THF solvents, an observation taken as evidence that the role of the solvent in this carbonylation is one of direct attack of the donor solvent at the metal center occurring concurrently with alkyl migration. This function of the solvent is less likely for insertion processes involving anionic RM(CO)₅⁻ species. This is particularly true if we choose not to proceed via a 20e⁻ complex since there are no ligands present capable of accepting an electron pair in order to accommodate

(47) Cotton, F. A.; Darensbourg, D. J.; Kolthammer, B. W. S.; Kudasroski, R. *Inorg. Chem.* **1982**, *21*, 1656.

(48) Darensbourg, D. J.; Kudasroski, R.; Delord, T. *Organometallics* **1985**, *4*, 1094.

(49) The k_{obsd} for CO₂ insertion into [PPN][CH₃Cr(CO)₅] in THF at ambient temperature and a total CO₂ pressure of 500 psi was determined to be 3.2 × 10⁵ s⁻¹.

(50) Darensbourg, D. J.; Grötsch, G. *J. Am. Chem. Soc.*, following paper in this issue.

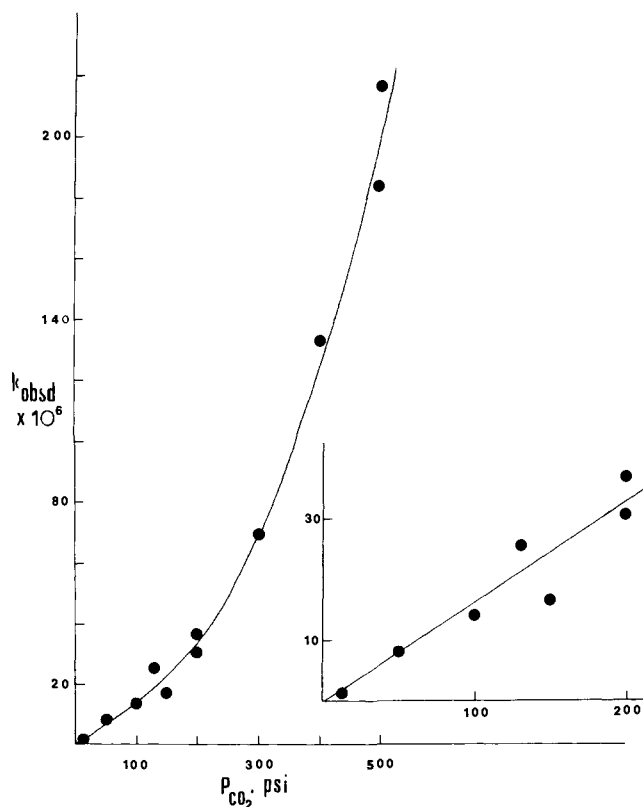


Figure 5. Plot of the pseudo-first-order rate constant (k_{obsd}) as a function of carbon dioxide pressure for the carboxylation of $\text{CH}_3\text{W}(\text{CO})_5^-$ in THF at 25 °C.

an associative (A) pathway, i.e., in the molybdenum species discussed above the $\eta^5\text{-C}_5\text{H}_5$ derivative can rearrange to an $\eta^3\text{-C}_5\text{H}_5$ species.⁵²⁻⁵⁴

Table VIII contains rate data for migratory CO insertion reactions of $\text{RW}(\text{CO})_5^-$ ($\text{R} = \text{CH}_3, \text{Et}, \text{Ph}$) at a variety of CO pressures. In parallel with kinetic studies involving $\text{RMn}(\text{CO})_5$ and $(\eta^5\text{-C}_5\text{H}_5)\text{Fe}(\text{CO})_2\text{R}$ derivatives, CO insertion into the $\text{R-W}(\text{CO})_5^-$ species displays significant retardation with decreasing electron-donating ability of the R substituent. As is indicated in Table VIII, migratory carbon monoxide insertion in $\text{EtW}(\text{CO})_5^-$ to afford $\text{EtC}(\text{O})\text{W}(\text{CO})_5^-$ occurs with a rate constant equal to $3.3 \times 10^{-4} \text{ s}^{-1}$ at 1 atm carbon monoxide pressure and ambient temperature. This, however, is not the limiting rate, for at higher carbon monoxide pressures (>100 psi) the reaction is complete upon mixing and spectral recording (<10 min). Hence, a conservative lower limit for k_1 is $5 \times 10^{-3} \text{ s}^{-1}$. This rate constant is much greater, at least an order of magnitude, than $k_2[\text{CO}_2]$ (k_{obsd} in Table VII) for carbon dioxide insertion in $\text{EtW}(\text{CO})_5^-$ at a CO_2 pressure of 400 psi. Dramatic illustration of this preference for the $\text{EtW}(\text{CO})_5^-$ derivative to undergo migratory carbon monoxide insertion instead of carbon dioxide insertion is seen in an experiment involving partial pressures of CO_2 and CO of 200 psi for each, where the acyl species is afforded exclusively (see Figure 6).

On the other hand, for CO_2 and CO insertion processes involving $\text{CH}_3\text{W}(\text{CO})_5^-$ $k_2[\text{CO}_2]$ and k_1 are comparable over a moderate range of CO_2 pressures. That is, $k_1(\text{av}) = 4.83 \times 10^{-5} \text{ s}^{-1}$ and $k_2[\text{CO}_2]$ varies from 1.38×10^{-5} to $2.00 \times 10^{-4} \text{ s}^{-1}$ over a 100 to 500 psi CO_2 pressure variation. Scheme I describes the two concurrent insertion processes which can take place in $\text{RW}(\text{CO})_5^-$ derivatives in the presence of carbon dioxide/carbon monoxide. The relative quantities of $\text{RCO}_2\text{W}(\text{CO})_5^-$ vs $\text{RCOW}(\text{CO})_5^-$ will depend on the ratio of $k_2[\text{CO}_2]$ to k_1 (at high CO pressures). As was noted for the CO_2 insertion process, CO

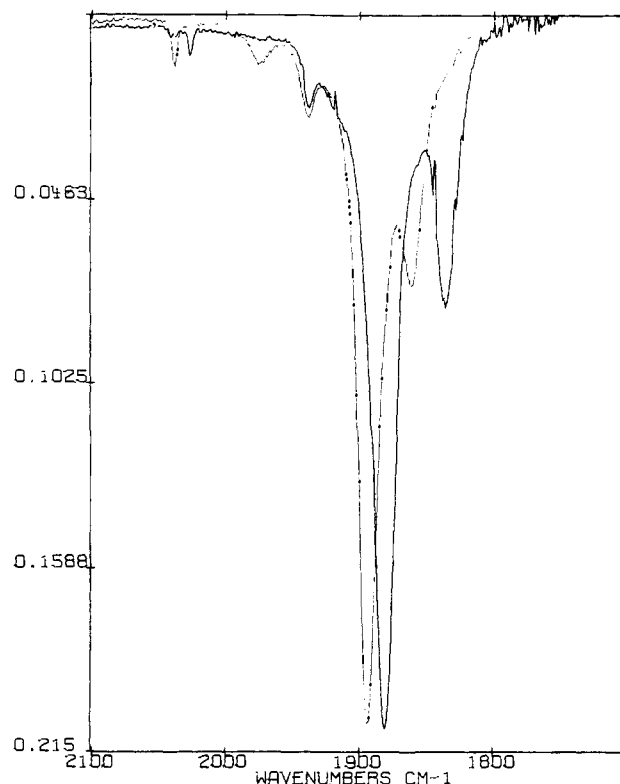
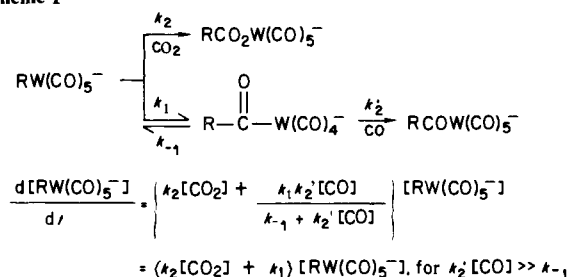


Figure 6. Infrared spectral traces in the $\nu(\text{CO})$ region for the reaction of $\text{EtW}(\text{CO})_5^-$ with CO_2/CO (20 psi each) in THF at 25 °C. Lighter trace due to $\text{EtCOW}(\text{CO})_5^-$ with peaks at 2038 (w), 1894 (s), and 1862 (m) cm^{-1} .

Scheme I



insertion involving these anionic species occurs with retention of configuration at the α -carbon center.⁵⁰

Consistent with the above analysis, the reaction of $\text{CH}_3\text{W}(\text{CO})_5^-$ with a mixture of carbon dioxide/carbon monoxide under conditions where the values of $k_2[\text{CO}_2]$ and $k_1 k_2'[\text{CO}]/(k_{-1} + k_2'[\text{CO}])$ are nearly equal resulted in the formation of an approximately equal mixture of $\text{CH}_3\text{CO}_2\text{W}(\text{CO})_5^-$ and $\text{CH}_3\text{COW}(\text{CO})_5^-$. Figure 7 contains infrared traces in the $\nu(\text{CO})$ region during the insertion process. Because of the similarity of the $\nu(\text{CO})$ vibrations of the starting material, $\text{CH}_3\text{W}(\text{CO})_5^-$, and the products of insertion, $\text{CH}_3\text{CO}_2\text{W}(\text{CO})_5^-$ and $\text{CH}_3\text{COW}(\text{CO})_5^-$, it was necessary to perform an infrared band-shape analysis to deconvolute the grossly overlapping band pattern. Once this is accomplished precise rate data for the disappearance of $\text{CH}_3\text{W}(\text{CO})_5^-$ with time are obtainable (see Figure 8). The pseudo-first order rate constant derived from such an analysis is $6.44 \pm 0.12 \times 10^{-5} \text{ s}^{-1}$, a value quite close to the sum of the individually acquired rate parameters, i.e., $k_2[\text{CO}_2] + k_1 k_2'[\text{CO}]/(k_{-1} + k_2'[\text{CO}])$ (see Tables V and VIII).

As would be anticipated on the basis of the independently determined rate data for CO_2 and CO insertion in the $\text{PhW}(\text{CO})_5^-$ species (Tables VII and VIII), when this derivative is reacted with a 400 psi pressure each of CO_2 and CO, tungsten pentacarbonyl benzoate is the predominant product. Furthermore, the rate of formation of $\text{PhCO}_2\text{W}(\text{CO})_5^-$ is approximately the same as that

(52) Darenbourg, D. J. *Adv. Organomet. Chem.* **1982**, *21*, 113.

(53) Basolo, F. *Inorg. Chim. Acta* **1981**, *50*, 65.

(54) Casey, C. P.; Jones, W. D. *J. Am. Chem. Soc.* **1980**, *102*, 6156.

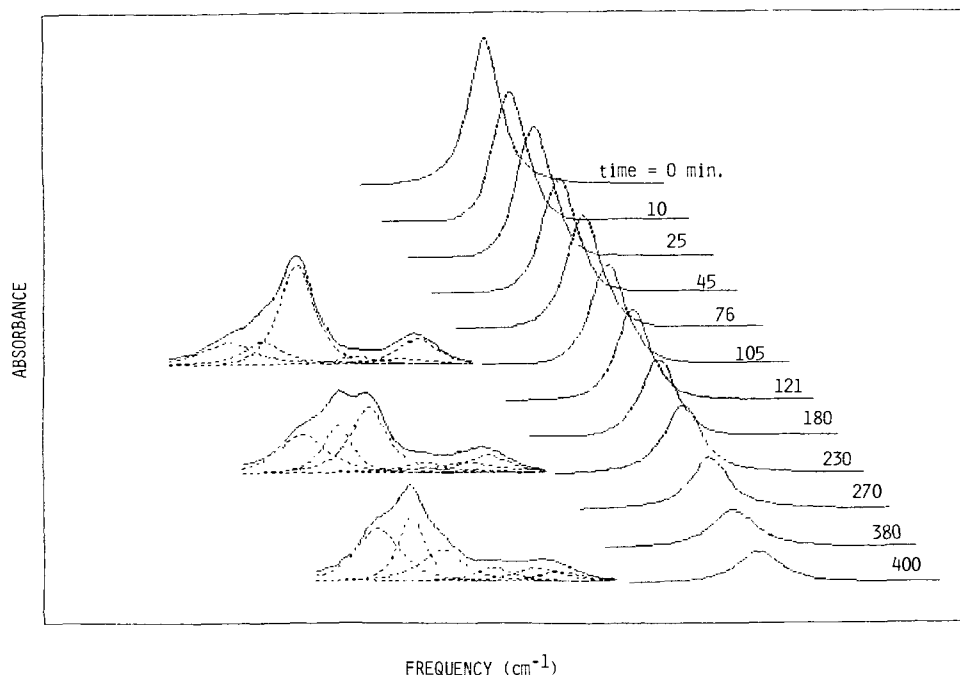


Figure 7. Time-dependent infrared spectra in the $\nu(\text{CO})$ region for the reaction of $\text{CH}_3\text{W}(\text{CO})_5^-$ with CO_2/CO (200 psi each) in THF at 25 °C. Deconvoluted spectra for the three significant species present, $\text{CH}_3\text{W}(\text{CO})_5^-$, $\text{CH}_3\text{CO}_2\text{W}(\text{CO})_5^-$, and $\text{CH}_3\text{COW}(\text{CO})_5^-$, shown at several stages of reaction.

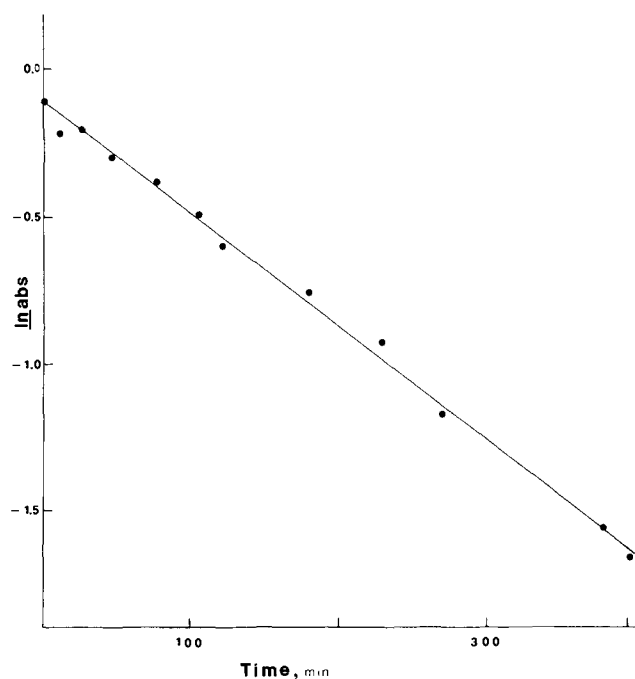


Figure 8. Rate plot for the disappearance of $\text{CH}_3\text{W}(\text{CO})_5^-$ in the reaction with CO_2/CO . Reaction was followed by monitoring the major band in $\text{CH}_3\text{W}(\text{CO})_5^-$ at 1883 cm^{-1} , where absorbances were taken from the deconvoluted band analysis.

observed at 400 psi of CO_2 in the absence of carbon monoxide.

It has been established that the rate of migratory CO insertion in the $\text{RMn}(\text{CO})_5$ species is not greatly influenced by prior substitution at the manganese center by phosphines.⁵⁵ This observation coupled with our note of a greatly accelerated CO_2 insertion reaction accompanied with phosphine substitution led us to repeat the reaction carried out above involving $\text{CH}_3\text{W}(\text{CO})_5^-$ with the identical CO_2/CO mixture employing *cis*- $\text{CH}_3\text{W}(\text{CO})_4\text{PMe}_3^-$ as substrate. The sole product from this reaction was *cis*- $\text{CH}_3\text{CO}_2\text{W}(\text{CO})_4\text{PMe}_3^-$, a result indicative of a greater

(55) Ruszczyk, R. J.; Huang, B.-L.; Atwood, J. D., personal communication. Results submitted for publication.

Table IX. Summary of Mechanistic Aspects of Carbonylation vs. Carboxylation Reactions

reaction variables	carboxylation	carbonylation ^a
kinetic order in CO_2 or CO	first order in CO_2	mixed order in CO; independent of CO at high CO pressures
nature of metal	third row more reactive than first row	first row more reactive than third row
R dependence	small dependence on R group, alkyls faster than aryls	reaction greatly retarded by electron-withdrawing R substituents
ancillary ligands	sterically nonencumbering phosphorus donor ligands greatly accelerate reaction	little effect
stereochemistry at α -carbon	retention of configuration	retention of configuration

^a These observations have been extensively noted for $\text{RMn}(\text{CO})_5$, and the more limited study on the group 6b anionic analogues reported herein is in complete agreement with these generalizations.

rate enhancement for CO_2 insertion over CO insertion upon increasing the electron density at the metal center via phosphine substitution.

Summary

A comparative summary of mechanistic aspects of carbonylation vs. carboxylation reactions is furnished in Table IX. Although there are some similarities in these two processes, there are some striking differences. These dissimilarities (dependences on metal, R group, and ancillary ligands) can be exploited in preferentially effecting carbon-carbon bond-forming processes involving carbon dioxide in the presence of carbon monoxide. The consequences of these mechanistic differences are of major importance in catalytic processes designed to utilize carbon dioxide as a C_1 feedstock.

Acknowledgment. The financial support of this research by the

National Science Foundation (Grant CHE 83-08281) is greatly appreciated.

Supplementary Material Available: A listing of observed and calculated structure factor amplitudes, ORTEP of the PPN⁺ cation

with the atomic labeling scheme, a complete listing of all bond lengths and angles for the cation, and tables of atomic positional coordinates and anisotropic thermal parameters for the cation (27 pages). Ordering information is given on any current masthead page.

Stereochemical Studies of the Carbon Dioxide Insertion Reactions into the Tungsten-Alkyl Bond

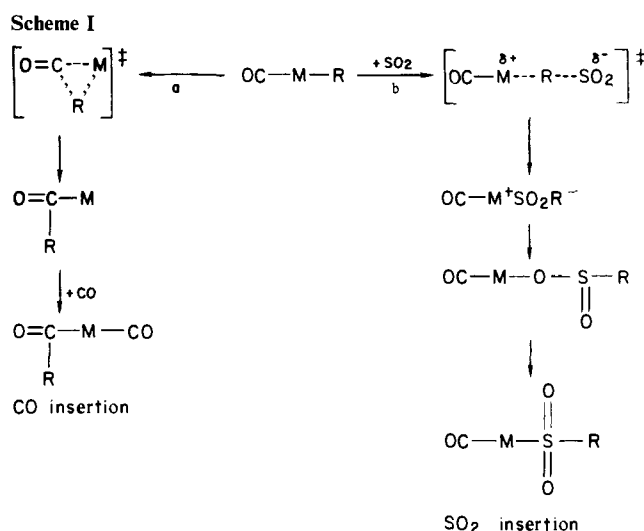
Donald J. Darensbourg* and Georg Grötsch

Contribution from the Department of Chemistry, Texas A&M University, College Station, Texas 77843. Received June 17, 1985

Abstract: Unequivocal demonstration of the α -carbon stereochemistry in the carbon dioxide insertion reaction has been accomplished by the conversion of *threo*-W(CO)₅CHDCHDPh⁻ with CO₂ to *threo*-W(CO)₅O₂CCHDCHDPh⁻, indicating that a high degree of retention of configuration at the carbon was involved. A similar observation has been noted for the phosphine substituted derivative *threo-cis*-W(CO)₄[PMe₃]CHDCHDPh⁻ which reacts with carbon dioxide to afford *threo-cis*-W(CO)₄[PMe₃]O₂CCHDCHDPh⁻. For comparative purposes, migratory CO insertion induced by carbon monoxide transformed *threo*-W(CO)₅CHDCHDPh⁻ to *threo*-W(CO)₅C(O)CHDCHDPh⁻. Hence, *threo*-W(CO)₅CHDCHDPh⁻ undergoes both insertion of carbon monoxide and carbon dioxide to afford 1,1- and 1,2-addition products, respectively, with retention of configuration at the α -carbon atom.

Mechanistic pathways of CO- and SO₂-insertion reactions into metal-carbon bonds have been extensively investigated over the past decade.¹ Examination of the stereochemical fate of the metal center² as well as the α -carbon^{3,4} has demonstrated that (a) CO insertion occurs with retention of configuration at the α -carbon atom and inversion of configuration at the metal center and (b) SO₂ insertion occurs with inversion of configuration at the carbon center and retention of configuration at the metal fragment. These stereochemical studies for CO insertion are indicative of a concerted 1,2-migration of the alkyl group to coordinated CO followed by the saturation of the free coordination site by the incoming nucleophile, e.g., CO.⁵ On the other hand, an S_E2 mechanism with SO₂ attacking at the backside of the alkyl group is operative for SO₂ insertion. These two quite different reaction pathways are diagrammatically illustrated in Scheme I below.

Stereochemical investigations of the less well-studied carbon dioxide insertion reaction into metal-carbon bonds⁶ have thus far not been reported, and the available kinetic and structural data



(1) (a) Wojcicki, A. *Acc. Chem. Res.* **1971**, *4*, 344. (b) Kitching, W.; Fong, C. W. *Organomet. Chem. Rev., Sect. A* **1970**, *5*, 281. (c) Jacobson, S. E.; Wojcicki, A. *J. Am. Chem. Soc.* **1973**, *95*, 6962. (d) Wojcicki, A. *Adv. Organomet. Chem.* **1973**, *11*, 88; **1974**, *12*, 32. (e) Calderazzo, F. *Angew. Chem.* **1977**, *89*, 305; *Angew. Chem., Int. Ed. Engl.* **1977**, *16*, 299. (f) Flood, T. C. *Top. Stereochem.* **1980**, *12*, 37. (g) Alexander, J. In "Chemistry of the Metal-Carbon Bond Stage 2"; Patai, S., Hartley, F. R., Eds.; Wiley: New York, 1983. (h) Kuhlmann, E. J.; Alexander, J. J. *Coord. Chem. Rev.* **1980**, *33*, 195. (i) Berke, H.; Hoffmann, R. *J. Am. Chem. Soc.* **1978**, *100*, 7224.

(2) (a) Flood, T. C.; DiSanti, F. J.; Miles, D. L. *Inorg. Chem.* **1976**, *15*, 1910. (b) Attig, T. G.; Wojcicki, A. *J. Am. Chem. Soc.* **1974**, *96*, 262. (c) Miles, S. L.; Miles, D. L.; Bau, R.; Flood, T. C. *J. Am. Chem. Soc.* **1978**, *100*, 7278.

(3) (a) Dong, D.; Slack, D. A.; Baird, M. C. *J. Organomet. Chem.* **1978**, *153*, 219. (b) Su, S.-C. H.; Wojcicki, A. *Organometallics* **1983**, *2*, 1296.

(4) Bock, P. L.; Boschetto, D. J.; Rasmussen, J. R.; Demers, J. P.; Whitesides, G. M. *J. Am. Chem. Soc.* **1974**, *96*, 2814.

(5) (a) Noack, K.; Calderazzo, F. *J. Organomet. Chem.* **1967**, *10*, 101. (b) Brunner, H.; Strutz, J. Z. *Naturforsch., B*, **1974**, *29*, 446. (c) Nicholas, K. M.; Rosenblum, M. *J. Am. Chem. Soc.* **1973**, *95*, 4449. Egglestone, D. L.; Baird, M. C.; Lock, C. J. L.; Turner, G. *J. Chem. Soc., Dalton Trans.* **1977**, 1576.

(6) (a) Braunstein, P.; Matt, D.; Dusausay, Y.; Fischer, J.; Mitschler, A.; Ricard, L. *J. Am. Chem. Soc.* **1981**, *103*, 5115. (b) Tsuda, T.; Chujo, Y.; Saegusa, T. *J. Am. Chem. Soc.* **1980**, *102*, 431. (c) Haggin, J. *Chem. Eng. News* **1982**, Feb 8, 13.

do not allow for a *definitive* assessment of the insertion process.⁷

In this paper, we wish to report on the stereochemistry at the α -carbon of the carbon dioxide insertion reaction into the tungsten-carbon bond. For convenience, we have chosen the [PNP][*cis*-W(CO)₄(L)(CHDCHDPh)] (L = CO and Me₃P) derivatives for these investigations since it is anticipated that the reaction pathway will be easily monitored by ¹H NMR spectroscopy⁸ and that the mechanistic analogy with other group 6 metal-alkyl and -aryl complexes will be maintained.⁹ An equally

(7) (a) Eisenberg, R.; Hendriksen, D. E. *Adv. Catal.* **1979**, *28*, 79. (b) Sneed, R. P. A. In "Comprehensive Organometallic Chemistry"; Wilkinson, G., Stone, F. G. A., Abel, E. W., Eds.; Pergamon Press: Oxford, 1982; Vol. 8, p 225. (c) Ito, T.; Yamamoto, A. "Organic and Bio-Organic Chemistry of Carbon Dioxide"; Inoue, S., Yamazaki, N., Eds.; Kodonsha, Ltd.: Tokyo, 1982; p 79. (d) Darensbourg, D. J.; Kudarski, R. *Adv. Organomet. Chem.* **1984**, *22*, 129.

(8) (a) Whitesides, G. M.; Boschetto, D. J. *J. Am. Chem. Soc.* **1971**, *93*, 1529; **1969**, *91*, 4313. (b) Dunham, N. A.; Baird, M. C. *J. Chem. Soc., Dalton Trans.* **1975**, 774. (c) Slack, D. A.; Baird, M. C. *J. Am. Chem. Soc.* **1976**, *98*, 5539.